



## COB-2021-0387

# THERMOPHYSICAL PROPERTIES CHARACTERIZATION OF MoS<sub>2</sub>/H<sub>2</sub>O-EG FOR HEAT TRANSFER APPLICATIONS

Felipe Silva dos Santos<sup>1</sup>

Edwin Martín Cardenas Contreras<sup>2</sup>

Enio Pedone Bandarra Filho<sup>3</sup>

Federal University of Uberlandia (UFU), School of Mechanical Engineering, Av. Joao Naves de Ávila, 2121 – Santa Monica, Uberlandia, MG 38400-902, Brazil

phelipe.moutinho@gmail.com<sup>1</sup>

emcardenas.1989@gmail.com<sup>2</sup>

bandarra@mecanica.ufu.br<sup>3</sup>

Otavio de Toledo Patrocinio<sup>4</sup>

Federal University of Uberlandia (UFU), Institute of Chemistry, Av. Joao Naves de Ávila, 2121 – Santa Monica, Uberlandia, MG 38400-902, Brazil

otaviopatrocínio@ufu.br<sup>4</sup>

**Abstract.** Nanofluids are heat transfer fluids with potential to replace traditional fluids (water, ethylene glycol, oil, etc.) and largely used for thermal energy transport applications. As a two-dimensional material, molybdenum disulfide (MoS<sub>2</sub>) has drawn wide attention due to properties and application prospects. In this work were evaluated the stability and thermophysical properties for different low concentrations (0.02-0.1 wt.%) of molybdenum disulfide (MoS<sub>2</sub>) to a mixture of water-ethylene glycol H<sub>2</sub>O-EG (50:50 in vol.%) in the presence of stabilizing agent, with focus on the heat transfer application. Two-step preparation method was used to produce the samples, where solid particles are pre-synthesized for hydrothermal method, separated, dried and then dispersed in the base liquid of interest. For a complete dispersion and reduction of nanoparticles cluster size, ultrasonic stirring and magnetic vibration were available. The addition of surfactant can improve the stability of the suspensions due the improvement of electrostatic stability, however their use can modify the nanofluids thermophysical properties, ie. viscosity, specific mass and thermal conductivity. The viscosity and density of nanofluids were investigated at 20-50 °C and the thermal conductivity was measured using the transient hot-bridge method at 20-50 °C. The structural characterization of nanofluid samples was studied by obtaining the optical absorption spectra using the UV-Vis spectroscopy, at the same wavelength for different concentration of nanofluid, commonly utilized to determine the stability of the nanofluids by a linear relationship between the absorbance and the concentration which follow the Beer-Lambert Law. UV-Vis absorbance of a nanofluids samples is a direct relationship with weight concentration. The morphological structure was analyzed using SEM to determine the agglomeration of particles by showing the size, shape, and distribution within the nanofluid. From the experimental results obtained it was possible to conclude that due the long-term stability and high thermal conductivity identify the MoS<sub>2</sub>/H<sub>2</sub>O-EG as a favorable additive in thermal energy engineering.

**Keywords:** Molybdenum disulfide, heat transfer, stability, thermal conductivity, UV-Vis spectroscopy

## 1. INTRODUCTION

Molybdenum disulfide (MoS<sub>2</sub>), one of the representative transition metal chalcogenide layered compounds, has draw great attention due its superior performance and application prospects. MoS<sub>2</sub> involves very optimal thermal and chemical stabilities. It demonstrates applications as a catalyst and lubricant due to its unique properties like anisotropy, photo-corrosion resistance and chemical inertness. The good thermophysical features and great anti-friction properties of this structures making it another promising material as reinforcement for the cooling purposes of nanofluids.

Jun *et al.* (2003), investigated the synthesis of MoS<sub>2</sub> powder by hydrothermal method, a method of synthesis via chemical reactions in a sealed and heated solution above ambient temperature and pressure D. and C. (2010), using MoO<sub>3</sub> powder and Na<sub>2</sub>S with the Mo/S ratio of 1:3 as precursors in HCl solution. They concluded that the formation mechanism of MoS<sub>2</sub> crystallites is different when the concentration of precursors is different and the morphological characteristics of MoS<sub>2</sub> nanowires suggests that the growth is possibly controlled by volume diffusion.

Yaru *et al.* (2013), investigated synthesis of MoS<sub>2</sub> microsphere by hydrothermal reaction, in which thiourea (CS(NH<sub>2</sub>)<sub>2</sub>) was used as S-source and reducing agent, ammonium heptamolybdate ((NH<sub>4</sub>)<sub>6</sub>Mo<sub>7</sub>O<sub>24</sub>·4H<sub>2</sub>O) was used as Mo-source.

They also used cationic surfactant Cetyl Trimethyl Ammonium Bromide (CTAB), anionic surfactant Sodium Dodecyl Benzene Sulfonate (SDBS) and nonionic surfactant Polyvinyl Pyrrolidone (PVP) as dispersing agent separately to prevent the reunion and achieve a certain effect. They observed that compared with SDBS and PVP, CTAB has the best dispersion effect, and the influence mechanism of which could be supposed as electrostatic interaction and stereo-hindrance effect.

The use of polyvinylpyrrolidone (PVP) to obtain controlled composition and structural features of MoS<sub>2</sub> was reported by some researchers M. *et al.* (2015), Li *et al.* (2017) and Weili *et al.* (2018). These authors used surfactant-assisted hydrothermal processes were applied to synthesize MoS<sub>2</sub> samples with controllable morphologies and structures. PVP can serve as a surface stabilizer, growth modifier, nanoparticle dispersant, and reducing agent. As shown by M. *et al.* (2015), its role depends on the synthetic conditions. This dependence arises from the amphiphilic nature of PVP along with the molecular weight of the selected PVP.

Ajay *et al.* (2017), experimentally investigated the synthesis and tribological performance of microfluids developed using functionalized  $\mu$ -MoS<sub>2</sub>. The 0.25 vol.% MoS<sub>2</sub> microfluid results in almost 40 % reduction in friction, and 6 % reduction in wear when compared with the base oil. The enhanced anti-friction anti-wear behavior of the MoS<sub>2</sub> microfluid can be attributed to the formation of efficient boundary films by MoS<sub>2</sub> particles as revealed from the SEM and EDX analysis.

Nader *et al.* (2017), reported the fabrication and thermophysical properties evaluation of ethylene glycol (EG) based heat exchange fluids containing molybdenum disulfide nanoparticles (MoS<sub>2</sub> NPs). The use of surfactants was avoided and ultrasonic agitation was used for dispersion and preparation stable MoS<sub>2</sub> nanofluids. A thermal conductivity enhancement of 16.4 % was observed for nanofluids containing 1 wt.% MoS<sub>2</sub> nanoparticles while the maximum increase in viscosity of 9.7 % was obtained for the same nanofluid at 20 °C.

Furlan *et al.* (2018), presented a review about the research developments in metal matrix self-lubricating composites containing MoS<sub>2</sub> compiled from 1945 up to 2017. Diverse tribological tests' configurations and parameters, as well as environmental details, have been highlighted and the composites' performance concerning wear and friction presented. The evaluation of the influence of raw materials, e.g. particle size, amount and type of lubricants or additives, as well as processing parameters, e.g. heating rate, temperature, well time, atmosphere, etc. might support the understanding of the reaction mechanisms. The authors concluded that by the combination of an adequate selection of the raw materials and a strict control of the processing parameters, the production of metal matrix composites containing MoS<sub>2</sub> as the main lubricant phase may be possible.

Wei *et al.* (2019), investigated the lubrication mechanism of different additives with the observation of wear scar using GNS/MoS<sub>2</sub> nanoplates (GNS/MoS<sub>2</sub> NPs). MoS<sub>2</sub> was anchored on the surface of graphene sheets (GNS) with hydrothermal process and chemical vapor deposition to obtain GNS/MoS<sub>2</sub> nanoflowers (GNS/MoS<sub>2</sub>-NFs) and GNS/MoS<sub>2</sub> nanoplates (GNS/MoS<sub>2</sub> NPs). The friction coefficient and wear scar diameter of base oil were reduced by 42.8 % and 16.9 % with the introduction of 0.02 wt.% GNS/MoS<sub>2</sub>-NFs, while that can only be reduced by 37.6 % and 11.9 % with the addition of 0.02 wt.% GNS/MoS<sub>2</sub>-NPs. The superior performance of GNS/MoS<sub>2</sub>-NFs additive can be contributed to the special microstructure which developed the synergistic effect between GNS and MoS<sub>2</sub>. Due to the synergistic effect, a tribo-film composed of oxide layer was formed on the rubbing surface during the sliding process, which can protect the friction pairs and reduce friction and wear.

Vignesh *et al.* (2020), investigated two separated process of MoS<sub>2</sub> synthesis via sonication assisted liquid phase technique. The first process involves bath sonication of bulk MoS<sub>2</sub> dissolved in N-methyl 2-pyrrolidone (NMP) for five hours followed by centrifugation. The second process involves probe sonication for two-hours at room temperature. A comparative characterization study of the exfoliated MoS<sub>2</sub> nanosheets is performed by UV-Vis, photoluminescence (PL), and Raman analysis. The comparative photoluminescence studies of the exfoliated fewer layers of MoS<sub>2</sub> nanosheets showed the emission spectra has a significant intensity advancement in the bath and probe sonication sample.

Juan *et al.* (2021), investigated the MoS<sub>2</sub>/graphene hybrid was successfully synthesized by microwave assisted hydrothermal method. Both of the charge transfer resistance and the photocurrent are tuned in graphene modified MoS<sub>2</sub> by enhancing photocatalytic nature. The researchers reported that the appropriate modification of graphene can reach the maximum yield of hydrogen gas. In addition, the appropriate conditions, such as the concentration of 0.32 M formic acid and the MoS<sub>2</sub> photocatalyst with 0.8 wt.% graphene (MSG<sub>0.8</sub>) dose of 0.0013 g L<sup>-1</sup>.

Salam *et al.* (2021), studied the lubrication properties of the inorganic hollow fullerene-like (IF) molybdenum disulfide (MoS<sub>2</sub>) solid lubricant immersed into the porous alumina matrix. The authors fabricated IF-MoS<sub>2</sub> matrix as a self-lubricant composite, IF-MoS<sub>2</sub> nano-particles were synthesized by dispersion of ammonium tetra-thiomolybdate ((NH<sub>4</sub>)<sub>2</sub>MoS<sub>4</sub>) in an organic solvent, and vacuum impregnation and annealing were used to immerse IF-MoS<sub>2</sub> nanoparticles into the porous alumina matrix. The obtained self-lubricant composite characterized by the field emission scanning electron microscope (FESEM) demonstrated hollow fullerene-like structure of IF-MoS<sub>2</sub> nanoparticles on the porous alumina matrix, and the transmission electron microscopy (TEM) results revealed the morphology of laminated layers. The cross section of the composite revealed that the depth of the permeated IF-MoS<sub>2</sub> which acted as a magnetic cling to the porous alumina.

In the present work, was prepared MoS<sub>2</sub>/H<sub>2</sub>O-EG (50:50) with low concentrations (0.02-0.1 wt.%) of molybde-

num disulfide (MoS<sub>2</sub>) focused on stability and thermophysical properties. Polyvinylpyrrolidone (PVP) was added to the nanoparticles to improve the stability of the suspensions. To determine the stability of nanofluids, UV-Vis spectroscopy at the same wavelength for different concentration of nanofluid was used. SEM is used to determine the agglomeration of particles by showing the size, shape, and distribution within the nanofluid.

## 2. EXPERIMENTAL PROCEDURE

### 2.1 Preparation of MoS<sub>2</sub>/H<sub>2</sub>O-EG

Molybdenum disulfide (MoS<sub>2</sub>) was synthesized in Aqueous Na<sub>2</sub>S<sub>2</sub>O<sub>3</sub> (1.58 g, 0.010 mol) and Na<sub>2</sub>MoO<sub>4</sub> (1.21 g), prepared by dissolving MoO<sub>3</sub> (0.72 g, 0.005 mol) in 10 mL of 0.5 mol/L KOH solution, were added to an autoclave with 15 mL of 25 % aqueous hydrazine (N<sub>2</sub>H<sub>4</sub>)(4.2g) solution and stirred into a clear, colorless solution. This solution was transferred to an autoclave and maintained at 200 °C for 24 h. The resulting black solid, after being washed and dried, was crystallized at 350 °C for 9 h in a flowing high-pure N<sub>2</sub> atmosphere, in agreement with the methodology described by Tang *et al.* (2016).

The samples of nanofluids were realized using two-step method. The nanoparticles were acquired in powder and scattered in a mixture of deionized water and ethylene glycol (H<sub>2</sub>O-EG (50:50 in vol.%)). The pH of the nanofluids was adjusted in average to 9 by potassium hydroxide (KOH) before the samples were submitted in ultrasonic bath for 15 min. The mixture was sonicated for 90 min with a power of 200 W at room temperature to enhance the dispersion of the nanoparticle in the base fluid. Figure 1 shows the described routine established.

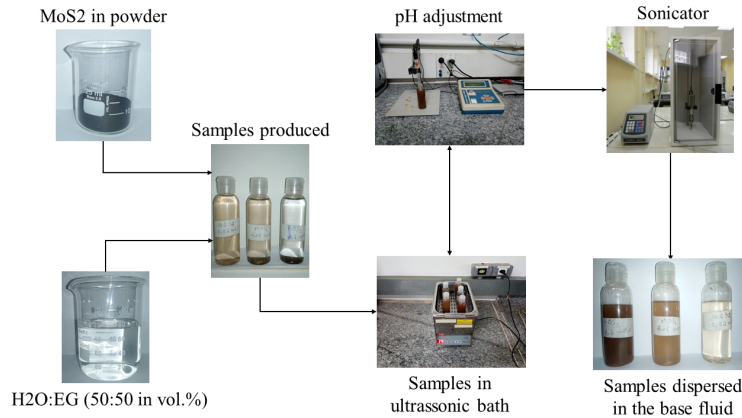


Figure 1. Nanofluid production process.

Table 1 shows the main properties of the samples produced as base fluid and mass concentration, to determine the amount of mass of nanoparticles a routine was developed in the EES software. In this sense, the desired volumetric concentration for each nanofluid and the final volume ( $V_f = 70$  ml) were previously defined.

Table 1. Description of nanofluid samples produced.

Nanoparticle	Diameter [nm]	Base Fluid [vol. %]	Mass Concentration [wt. %]
MoS <sub>2</sub>	300-500	H <sub>2</sub> O-EG (50:50)	0.02
			0.05
			0.1

Eq. (1) shows the calculus routine for the mass concentration, were computed 3 different mass concentration of MoS<sub>2</sub> (0.02 %, 0.05 % and 0.1 %) in the base fluid, H<sub>2</sub>O-EG (50:50), where  $m_{np}$  is the mass of nanoparticle and  $m_{bf}$  is the mass of base fluid.

$$wt.\% = \frac{m_{np}}{m_{np} + m_{bf}}, \quad (1)$$

Figure 2 shows the morphological structure of the samples obtained by SEM analysis to determine the agglomeration of particles by showing the size, shape, and distribution within the nanofluid.

### 2.2 Thermophysical properties

In this work, the thermal conductivity was measured by a conductivimeter LINSEIS, model THB-1, it is based in the hot transient bridge technique, which allows the measurement of thermal conductivity, thermal diffusivity and specific

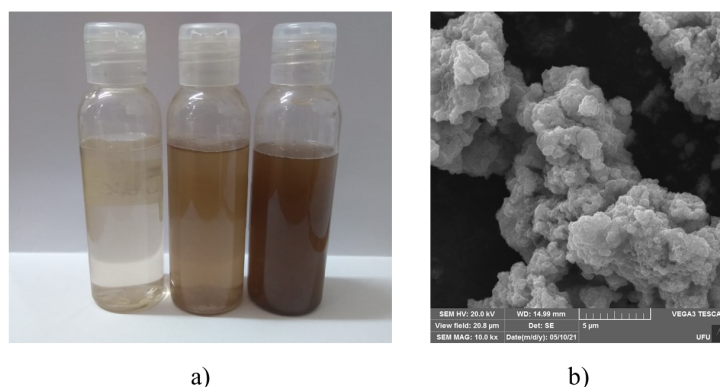


Figure 2. Morphological characterization. a) Samples of nanofluid; b) SEM image of MoS<sub>2</sub>/H<sub>2</sub>O-EG nanofluid.

heat of various materials as solids, liquids, powders and pastes. The measurement is automatic and did by the software provide by the manufacturer with 10 measurements per cycle and 2 to 3 cycles per sample. The range of temperatures used was 20 °C to 50 °C. Tab. 2 show the conductivimeter uncertainty range of measurement in detail.

Table 2. Properties of THB-1 LINSEIS conductivimeter provided by manufacturer.

Parameter	Temperature range	Measurement range	Measurement uncertainty
Thermal conductivity	20 °C to 50 °C	0.01 to 1 W/(mK)	Better than 2 %
Thermal diffusivity		0.05 to 10 mm <sup>2</sup> /s	Better than 5 %
Specific heat		100 to 5000 kJ/(m <sup>3</sup> K)	Better than 5 %

The temperature range used was 20 °C to 50 °C. The final value of conductivity was the arithmetic mean of results obtained, eliminating discrepant results.

The dynamic viscosity as well as the density of the nanofluids were measured on a rotational viscometer, model Stabinger<sup>TM</sup> SVM<sup>TM</sup> 3000, from Anton Paar, which has a cylindrical geometry with concentric tubes. The temperature was controlled by the equipment using a range 20 °C-80 °C. The samples were injected in the equipment, and the calculation of the dynamic viscosity did from the rotor speed. Simultaneously the equipment obtained values of dynamic viscosity, viscosity kinematics and specific mass. Tab. 3 presented the uncertainty measurements of viscosity, specific mass and temperature and its repeatability.

Table 3. Uncertainty data of Anton Paar viscometer measurement.

Parameter	Temperature range	Uncertainty	Repeatability
Dynamic viscosity	20 °C to 80 °C	± 0.35 %	± 0.1 % of measured value
Density		± 0.0005 %	± 0.0002 g/cm <sup>3</sup>
Temperature		± 0.02 %	± 0.0005 °C

### 2.3 Stability analysis

The stability of MoS<sub>2</sub>/H<sub>2</sub>O-EG nanofluid was studied by obtaining the optical absorption spectra using the UV-Vis spectroscopy. The peaks of wavelength ranging from 400-1100 nm were used to obtained the relationship of absorbance and mass concentration. A wavelength of 400 nm was used of reference value to show the relation between mass concentration and absorbance of samples, as can be seen how much higher the mass concentration, grater its absorbance. Fig. 3 shows the obtained values after preparation of samples. It was noted a linear relation between absorbance and mass concentration as reported by Swinehart (1962).

Figure 4 shows the results of UV-Vis spectroscopy in a reference wavelength value of 400 nm for relative mass concentration obtained of a linear regression by figure 3 in relation to different times of measurement.

The relative concentrations were obtained by a linear regression of the data in figure 3. Eq. 2 shows the linear regression obtained, where A is the absorbance and M is the mass concentration. Table 4 shows the absorbance of nanofluid samples for a reference wavelength value of 400 nm to different times of measurement and the results of this regression respectively. As can be observed the mass concentration decrease as time goes on, its happen probably due the decanting of samples, which leads to a decrease in absorbance over time.

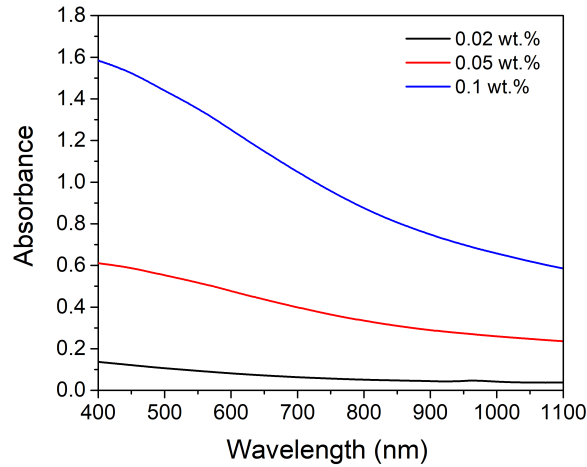


Figure 3. Relationship between absorbance and wavelength for nanofluid samples.

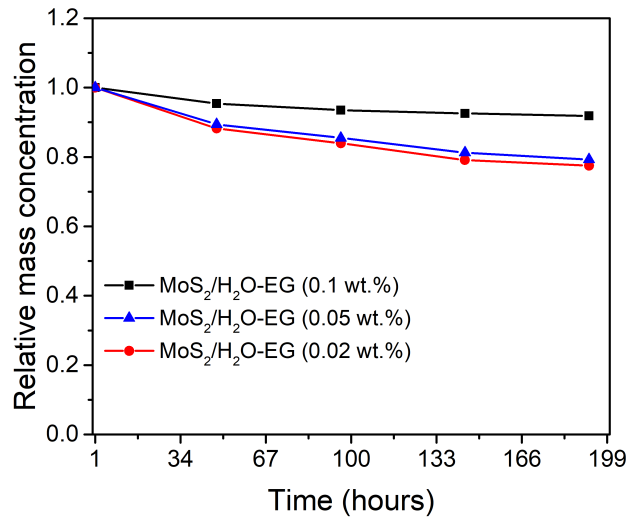


Figure 4. Relative wavelength of MoS<sub>2</sub>/H<sub>2</sub>O-EG nanofluid in relation to different times of measurements.

UV-vis spectroscopy is used to quantitatively characterize the stability of the dispersion of nanofluids samples due the easy visualization of wavelength decrement during the time. How much lower the wavelength decrease more stable is the nanofluid samples.

$$A = 18.237 \times M + 0.2559, \quad (2)$$

Table 4. Absorbance of nanofluids samples in different times of measurement.

	wt. %	1 hour	48 hours	96 hours	148 hours	192 hours
Absorbance	0.02	0.1369	0.1187	0.1114	0.1076	0.1049
	0.05	0.611	0.509	0.472	0.430	0.416
	0.1	1.5846	1.3896	1.3177	1.2393	1.2029

### 3. RESULTS

This section presents the experimental results of thermal conductivity, density and dynamic viscosity measurements for MoS<sub>2</sub>/H<sub>2</sub>O-EG nanofluid. A comparison with the physical properties of the theoretical base fluid was done for different temperature ranges in all analysed cases. Fig. 4 and Fig 5 shown the results of dynamic viscosity and specific mass for nanofluid using a temperature range of 20 °C-80 °C.

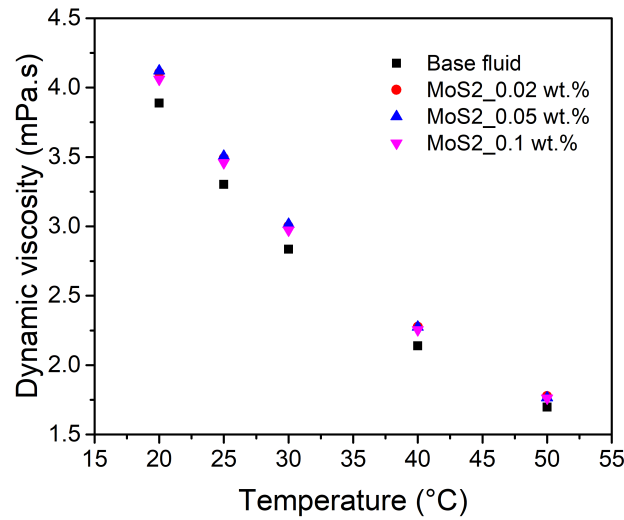


Figure 5. Comparison between experimental results for dynamic viscosity of nanofluid samples and base fluid.

In Fig. 5 we can see that the nanofluid samples present dynamic viscosity values higher than base fluid, where the maximum viscosity increments obtained for nanofluid samples of MoS<sub>2</sub>/H<sub>2</sub>O-EG were on average 6.39 %, 7.69 % and 6.80 % for nanofluid samples with mass concentration of 0.02 wt.%, 0.05 wt.% and 0.1 wt.%. The absorbed water layer can be formed around the nanoparticles in nanofluids, which increases the equivalent radius of nanoparticles. Higher interfacial resistance will form for higher surface area, which will hinder the mobility of the nanoparticles in base fluid, causing the increase in the viscosity (Zhang and Han (2018)).

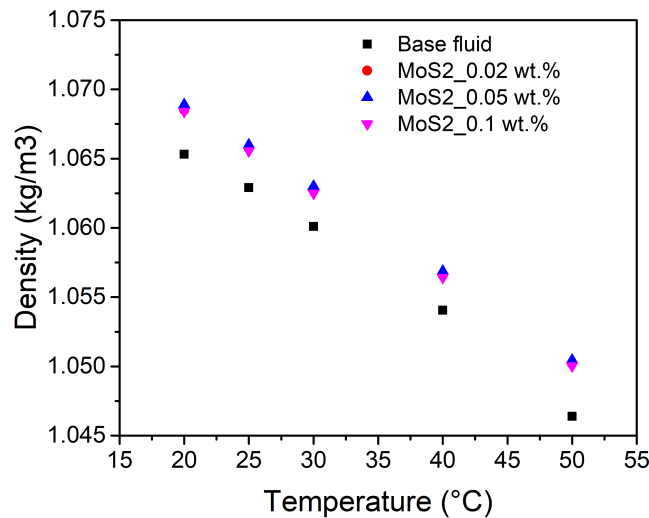


Figure 6. Comparison between experimental results for density of nanofluid samples and base fluid.

In Fig. 6 we can observe a slight increment of the density of nanofluid samples in relation to base fluid. The maximum increments obtained for nanofluid samples of MoS<sub>2</sub>/H<sub>2</sub>O-EG in relation to base fluid were on average 0.36 %, 0.39 % and 0.35 % for nanofluid samples with mass concentration of 0.02 wt.%, 0.05 wt.% and 0.1 wt.%. Due the attraction of van de Waals force existed among the particles of nanofluids, the nanoparticles are inclined to gather to form aggregate in nanofluids, and when the mass fraction of the nanoparticles in the nanofluids increase, the quantity of the nanoparticles will increase too, thus the nanoparticle tend to form bigger aggregate in the nanofluids.

Figure 7 shows the experimental results for thermal conductivity of MoS<sub>2</sub>/H<sub>2</sub>O-EG nanofluid samples in relation to different temperatures in a range of 20 °C-50 °C at which measurements were taken. With the increase in the temperature, the Brownian movement of nanofluids tends to get stronger, the average speed of each molecule increases and the contact time of the particles in the nanofluids decreases leading to reduction of the time interaction.

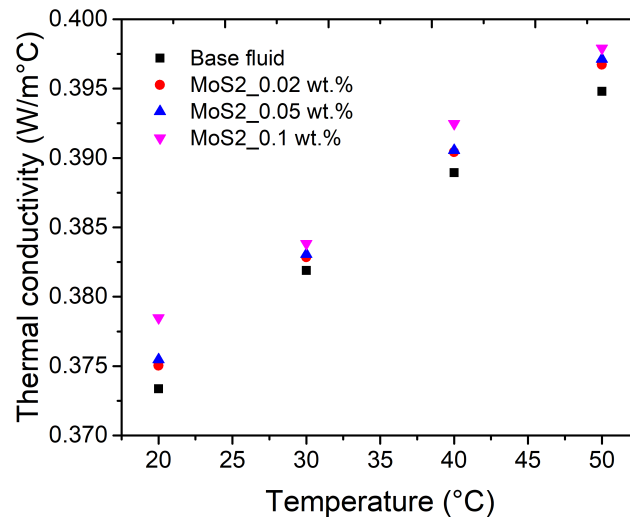


Figure 7. Thermal conductivity of MoS<sub>2</sub>/H<sub>2</sub>O-EG nanofluid in relation to different temperatures.

The maximum increment of temperatures obtained for nanofluid samples of MoS<sub>2</sub>/H<sub>2</sub>O-EG in relation to base fluid were on average 0.49 %, 0.59 % and 1.37 % for nanofluid samples with mass concentration of 0.02 wt.%, 0.05 wt.% and 0.1 wt.%. It is observed a slight increment of nanofluid thermal conductivity with the increase of temperature and with the increase of the volume concentration of nanoparticles. At high temperatures, the reduction of the surface energy of the nanoparticle is favored, reducing the possibility of nanoparticle agglomeration and causing a decrease in viscosity leading to an intensification of Brownian motion.

The enhancement of thermal conductivity was ~ 1 % on average, what is much lower than values obtained by Nikkam *et al.* (2019), using water/ethylene glycol as base fluid they obtained a thermal conductivity enhancement of ~ 12.4 % with ~ 10.6 % viscosity increase at 20 °C. The lower values obtained of thermal conductivity could be attributed to the particle morphological including shape, size and purity of base liquids as well as the surface chemistry of the particles. Su *et al.* (2015) showed thermal conductivity enhancement of < 1 % for nanofluids with both LB2000 oil and PriECO600 polyhydric alcohol at nanoparticles loading of 0.5 wt.%. They reported values closed to the values obtained for our fabricated nanofluids and much lower than the values obtained by Nikkam *et al.* (2019). The possible reason maybe again be related to the different morphology including size and shape, dissimilar surface chemistry and presence of impurities can be some possible reasons for this difference. Thus this study indicates that MoS<sub>2</sub>/H<sub>2</sub>O-EG can be an efficient heat transfer fluid for various applications.

#### 4. CONCLUSIONS

The results show that the enhancement obtained by the MoS<sub>2</sub>/H<sub>2</sub>O-EG nanofluid in comparison with the base fluid was lower than we expected, one reason can be the indetermination of the nanofluid isoelectric point to enhancing or decrease the pH value of substance, which could help the improve the performance of the nanofluid in terms of thermal conductivity. UV-Vis spectroscopy show that with the increase of temperature and volume concentration, the thermal conductivity was slightly increase due the reduction of the surface energy of nanoparticle favorable by high temperatures, what cause a decrease in viscosity leading to an intensification of Brownian motion. As observed by Zhang and Han (2018) the van der Waals attractive force of the nanofluid particles increases with the increasing mass fraction of nanoparticles, so the viscosity of nanofluids increases with the increasing mass fraction of nanoparticles. Due the long-term stability and high thermal conductivity MoS<sub>2</sub>/H<sub>2</sub>O-EG is identify as a favourable additive in thermal energy engineering, however more studies are necessary to verify the main advantages in terms of thermal performance gains in relation to conventional heat transfer fluids.

#### 5. ACKNOWLEDGEMENTS

The authors are grateful for the financial support provided for this research by CAPES and CNPq.

## 6. REFERENCES

- Ajay, K., D., T.G., K., A.P., S., K.L.N., S., S., Raghuvir, S. and K., J.A., 2017. “Experimental study on the efficacy of mos<sub>2</sub> microfluids for improved tribological performance”. *Proceedings of the Institution of Mechanical Engineers, Part J: Journal of Engineering Tribology*, Vol. 231, No. 0, pp. 107–124.
- D., L.A. and C., L.W., 2010. “Optical properties of ferroelectric nanocrystal/polymer composites”. *Physical Properties and Applications of Polymer Nanocomposites*, Vol. 0, No. 0, pp. 108–158.
- Furlan, K.P., de Mello, J.D.B. and Klein, A.N., 2018. “Self-lubricating composites containing mos<sub>2</sub>: A review”. *Tribology International*, Vol. 120, pp. 280–298.
- Juan, L.G., Hong, H.Y., Yi, C.C., Yie, T.C., Cheng, C.Y., Heng, C.J., Leng, H.T., Sambandam, A. and J., W.J., 2021. “Enhanced performance for photocatalytic hydrogen evolution using mos<sub>2</sub>/graphene hybrids”. *International Journal of Hydrogen Energy*, Vol. 225, No. 8, pp. 5938–5948.
- Jun, L.W., Wei, S.E., Min, K.J., Zhan, C.Z., H., O. and Tsuguo, F., 2003. “Hydrothermal synthesis of mos<sub>2</sub> nanowires”. *Journal of Crystal Growth*, Vol. 250, No. 0, pp. 418–422.
- Li, M., Wang, D., Li, J., Pan, Z., Ma, H., Jiang, Y., Tian, Z. and Lu, A., 2017. “Surfactant-assisted hydrothermally synthesized mos<sub>2</sub> samples with controllable morphologies and structures for anthracene hydrogenation”. *Chinese Journal of Catalysis*, Vol. 38, pp. 597–606.
- M., K.K., Stefanos, M., Lakshminarayana, P., E., S.S., M., K.K., Stefanos, M., Lakshminarayana, P. and E., S.S., 2015. “Polyvinylpyrrolidone (pvp) in nanoparticle synthesis”. *Royal Society of Chemistry*, Vol. 44, No. 0, pp. 17883–17905.
- Nader, N., S., T.M., Joydeep, D., Mohammed, A.A., Zar, M.M.T., Maissa, S. and Majid, M.S., 2017. “Fabrication and thermo-physical properties characterization of ethylene glycol—mos<sub>2</sub> heat exchange fluids”. *International Communications in Heat and Mass Transfer*, Vol. 89, No. 0, pp. 185–189.
- Nikkam, N., Dutta, J., Al-Abri, M., Myint, M.T.Z. and Toprak, M.S., 2019. “Influence of the base liquid and particle size on the thermo-physical characteristics of mos<sub>2</sub> micro and nanofluids”. *Heat and Mass Transfer Research Journal*, Vol. 3, No. 1, pp. 73–82.
- Salam, A., Xie, G., Guo, D. and Xu, W., 2021. “Fabrication and tribological behavior of self-lubricating composite impregnated with synthesized inorganic hollow fullerene-like mos<sub>2</sub>”. *Composites Part B*, Vol. 207, pp. 1–10.
- Su, Y., Gong, L., Li, B. and Chen, D., 2015. “An experimental investigation on thermal properties of molybdenum disulfide nanofluids”. In *Proceedings of the 2015 International Conference on Materials, Environmental and Biological Engineering*. Guilin, China.
- Swinehart, D.F., 1962. “The beer-lambert law”. *Journal of Chemical Education*, Vol. 39, No. 7, pp. 333–335.
- Tang, H., Huang, H., Wang, X., Wu, K., Tang, G. and Li, C., 2016. “Hydrothermal synthesis of 3d hierarchical flower-like mos<sub>2</sub> microspheres and their adsorption performances for methyl orange”. *Applied Surface Science*, Vol. 379, pp. 296–303.
- Vignesh, Siddharth, K., K., T.U., Kant, C.R., Kamaldeep, S. and K., S.R., 2020. “Study of sonication assisted synthesis of molybdenum disulfide (mos<sub>2</sub>) nanosheets”. *Materials Today: Proceedings*, Vol. 21, No. 0, pp. 1969–1975.
- Wei, S., Jincan, Y. and Hongbing, J., 2019. “Fabrication of gns/mos<sub>2</sub> composite with different morphology and its tribological performance as a lubricant additive”. *Applied Surface Science*, Vol. 469, No. 0, pp. 226–235.
- Weili, W., Bingqing, Q., Chenxi, L., Xiaqiang, S., Jing, T., Yi, L. and Guokun, L., 2018. “Pvp functionalized marigold-like mos<sub>2</sub> as a new electrocatalyst for highly efficient electrochemical hydrogen evolution”. *Electrocatalysis*, Vol. 11, No. 4, pp. 280–298.
- Yaru, C., Jiangshan, H., Xiaoming, L., Junxue, Z., Aoli, C. and Jun, Y., 2013. “Preparation and characterization of mos<sub>2</sub> microsphere by hydrothermal method”. *Advanced Materials Research*, Vol. 0, No. 0, pp. 306–309.
- Zhang, S. and Han, X., 2018. “Effect of different surface modified nanoparticles on viscosity of nanofluids”. *Advances in Mechanical Engineering*, Vol. 10, pp. 1–8.

## 7. RESPONSIBILITY NOTICE

The authors are solely responsible for the printed material included in this paper.